Electronic Supplementary Material (ESI) for ChemComm.

Supporting Information

Self-assembly of molecular ions via anti-electrostatic hydrogen bonds (AEHB) and through-space defined organic domains

Joshua S. McNally[a], Xiaoping Wang[b], Christina Hoffmann[b], and Aaron D. Wilson*[a]

Table of Contents

Figures and Tables

S1. Solution Preparation and Methods

Deionized water was used for these experiments. The tertiary amine to carbonic acid stoichiometry for a saturated solution used in Figure 1 and S1 has been previously reported[1,2] or collected as previously reported[1]. Tertiary amines were obtained from Aldrich and used as received. All equipment was used in accordance with manufacturer speciation unless stated otherwise.

S1.1. Production of tertiary ammonium bicarbonate solutions

As an example, deionized water (3.884 g) and dimethylhexylamine (6, 5.468 g, 7.35 ml, 0.0423 mol) are placed in home-built carbon dioxide addition cell.[1] The carbon dioxide addition cell was designed to measure the volume of nonpolar amine which remained phase separated from the aqueous volume. Knowing the original volume of the amine, it was possible to calculate the volume which had reacted with the known volume of water. The addition cell from bottom to top features a fine frit base with a 2.5 cm diameter, 5 ml reservoir bulb, 10 ml graduated cylinder (1.5 cm diameter 8 cm tall), 25ml reservoir bulb, 30 cm condenser. A small stir bar is added and stirred rapidly, the condenser is operated at 2 °C, and CO_2 is flowed through the cell at a steady rate of <3 ml s^{-1}. After a 50 min purge, 1.0 ml of the amine is unreacted, after 2 h 0.9 ml of the amine unreacted. The solution was purged with carbon dioxide for a total of 5 h with 0.9 ml of the amine unreacted. The product, approximately $[HN(Me)_2Cy\ HCO_3]$, and unreacted amine are removed with a syringe and long needle.

S1.2. NMR stoichiometry and concentration studies

Nuclear magnetic resonance (NMR) spectra were acquired on a Bruker Avance III 600 MHz spectrometer with a magnetic field strength of 14.093 Tesla, corresponding to operating frequencies of 600.13 MHz (^{1}H), and 150.90 MHz (^{13}C). All NMR were captured with a co-axial insert containing C_6D_6 (Cambridge Isotopes Laboratories). ^{1}H NMR spectra were collected with a 30° pulse and 10 s delays between scans, the T_1 of every integrated shift was verified, most T_1 relaxations well under 1 sand none above 2 s. The integration was set to a known peak in of the tertiary amine providing the relative concentration of (H_2O + H_2CO_3):tertiary amine. ^{13}C NMR spectra with quantifiable integration were obtained with inverse gated decoupling spectra with a 30° pulse and 60 second delays between scans. The ^{13}C T_1 values were verified and found to range between 2.5 s and 10.5 s for the carbonate peak, all other peaks had shorter relaxation times. The integration of the carbonate peaks was set to unity providing the relative concentration of tertiary amine:carbonate. Results are featured in Table S1 anf Figure S1.

S1.3. Dynamic Light Scattering Dynamic Light scattering experiments were conducted on aqueous dimethyl-*n*-octylamine carbonic acid solutions at various concentrations with a Zetasizer Nano S at 15 °C. The Nano S contains a 4 mW He-Ne laser operating at a wavelength of 633 nm and an avalanche photodiode dectector (APD). The scatter was detected at an angle of 173°.

Table S1. Saturated solution properties for various amines.

Molecule	Amine Carbon: Nitrogen Ratio	Amine: H_2CO_3 Ratio	wt%	Surface area beyond 0.45 nm, nm^2	First reported
Dimethylbutylamine	6	1.06	67.9	0.0145	1
Triethylamine	6	1.05	51.1	0.0000	1
1-Ethylpiperidine	7	1.05	70.6	0.0000	1
Methyldipropylamine	7	1.07	27.9	0.0000	1
Dimethylcyclohexylamine	8	1.05	77.1	0.0004	1
Dimethylhexylamine	8	1.23	64.1	0.1469	1
1-Butylpyrrolidine	8	1.26	63.4	0.0186	1
Diethylbutylamine	8	1.09	36.1	0.0621	1
Dimethylbenzylamine	9	1.14	31.9	0.0645	1
Methyldibutylamine	9	1.14	11.1	0.0012	1
Dimethylphenethylamine	10	2.42	70.6	0.1469	1
Dimethyloctylamine	10	1.91	65.9	0.2753	1
Diethylcyclohexylamine	10	1.02	34.8	0.0008	1
Dimethyl-2-ethylhexylamine	10	1.05	2.31	0.1607	1
Dimethylnonylamine	11	2.70	66.8	0.3368	1
1-Cyclohexylpiperidine	11	1.00	72.0	0.0026	2
Dimethyldecylamine	12	2.87	61.5	0.4131	1
1-Benzylpiperidine	12	1.04	17.5	0.0463	This Study
dicyclohexylmethylamine	13	1.06	59.7	0.0000	This Study

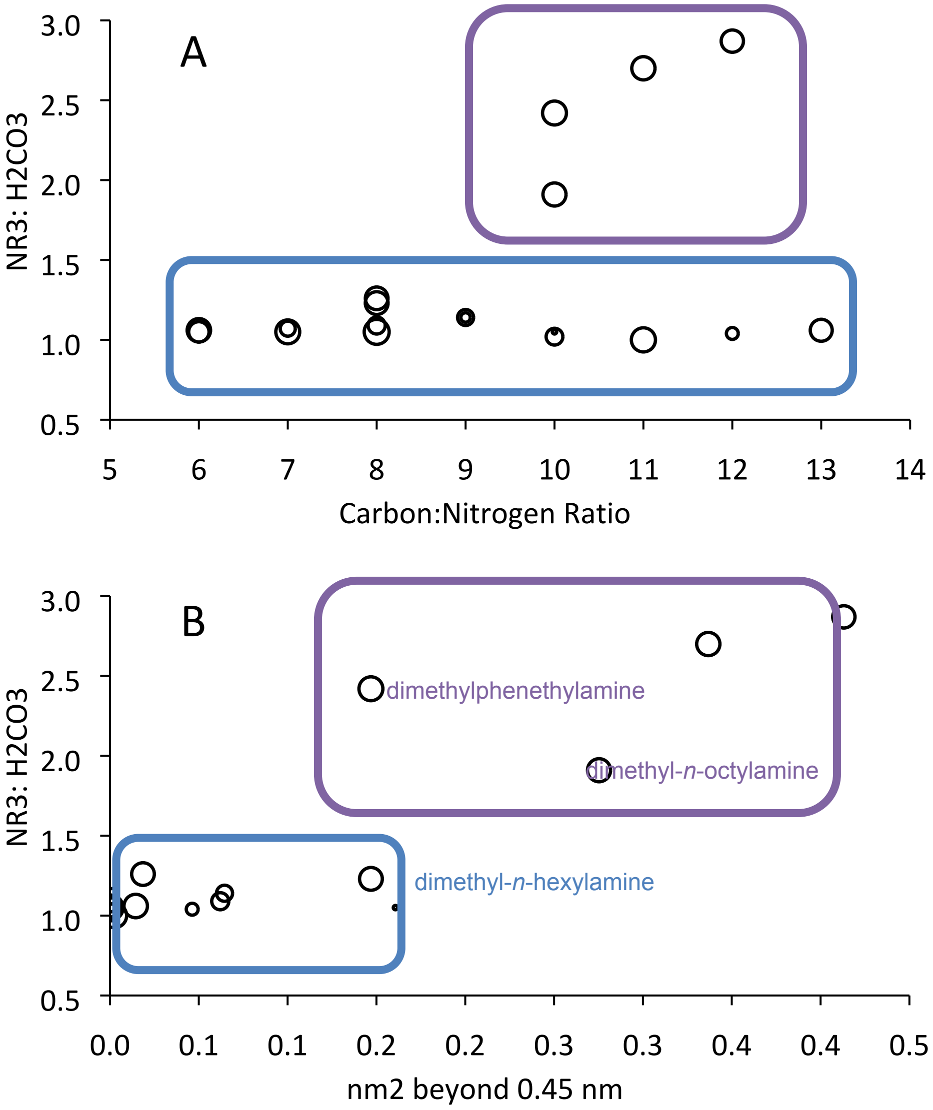

Figure S1. (A) Tertiary amine carbon to nitrogen ratio versus observed amine to carbonic acid stoichiometry for a saturated solution.[1] Circle size is defined by the weight percent concentration of amine and carbonic acid. (B) Tertiary organic domain, defined by the surface area outside a through-space sphere of 0.45 nm centered at the protonated nitrogen, versus amine to carbonic acid stoichiometry. (Identical to Figure 1 reproduced for convenience.)

S2. DFT Calculations All geometry optimizations and vibrational frequency calculations were carried out using Gaussian03 (Revision C.02).[3] The B3LYP functional, which uses Becke's three parameter exchange functional (B3) and the correlation function of Lee, Yang and Parr (LYP)[4–9] was used for all calculations. The valance triple-ζ 6-311++G(d,p) basis set was used, which includes polarization functions on all atoms and diffuse functions on non-hydrogen atoms. Frequency calculations performed at the B3LYP/6-311++G(d,p) level of theory confirmed energy minimized geometries with the absence of any imaginary frequencies. The geometric parameters associated with dimethylcyclohexylamine were obtained from the x-ray crystal structure data, which was solved as an asymmetric unit containing two pairs of the cation and anion (*vide infra*). The parameters of a single amine were geometry optimized to give an energy minimized structure.[10] The initial geometries of the remaining amines were generated using Gaussview (Revision 3.09), and then energy minimized. Surface area analyses were performed with the UCSF Chimera package. Chimera is developed by the Resource for Biocomputing, Visualization, and Informatics at the University of California, San Francisco (supported by NIGMS P41-GM103311).[11] The results have been used to generate data in Table S1 as well as Figure S1b and Figure 1b.

S3. Neutron Structure Data for **DMCHA** were collected on the TOPAZ single-crystal time-of-flight (TOF) Laue diffractometer at the Spallation Neutron Source, Oak Ridge National Laboratory[12]. A plate-shaped hydrogenated crystal of **DMCHA**, with dimensions of 0.20 x 1.50 x 1.55 mm was cut from a centimeter long crystal and mounted on the tip of a MiTeGen loop using Super Glue, and transferred to the TOPAZ goniometer for data collection at 100 K. To ensure good coverage and redundancy, data were collected using 25 crystal orientations optimized with CrystalPlan software[13] for an estimated 98% coverage of symmetry-equivalent reflections of the monoclinic cell. Each crystal orientation was measured for ~5 hr. The integrated raw Bragg intensities were obtained using the 3-D ellipsoidal Q-space integration by previously reported methods[14]. Data reduction including neutron TOF spectrum Lorentz and detector efficiency corrections was carried out with the ANVRED3 program. A Gaussian numerical absorption correction was applied with $\mu = 0.1858 + 0.1461\ \lambda\ \mathrm{cm}^{-1}$. The reduced data were saved in SHELX HKLF2 format in which the wavelength is recorded separately for each reflection. The initial neutron structure was refined starting from the X-ray structure using non-hydrogen C, N and O atom positions. The positions of H atoms were located in difference-Fourier maps from the subsequent refinement of the neutron data. The crystal structure was refined anisotropically to convergence using the SHELXL-2014 program[15] in WinGX[16]. CCDC 1532783 contains the supplementary crystallographic data. These data can be obtained free of charge from The Cambridge Crystallographic Data Centre.

S4. References

[1] A. D. Wilson, F. F. Stewart, *RSC Adv.* 2014, **4,** 11039–11049.
[2] C. J. Orme, A. D. Wilson, *Desalination* 2015, **371**, 126–133.
[3] M. Frisch, G. Trucks, H. Schlegel, G. Scuseria, M. Robb, J. Cheeseman, J. Montgomery, T. Vreven, K. Kudin, J. Burant, et al., 2004.
[4] S. H. Vosko, L. Wilk, M. Nusair, *Can. J. Phys.* 1980, **58**, 1200–1211.
[5] A. D. Becke, *Phys. Rev. A* 1988, **38**, 3098–3100.
[6] A. D. Becke, *The Journal of Chemical Physics* 1993, **98**, 5648–5652.
[7] A. D. Becke, *The Journal of Chemical Physics* 1992, **97**, 9173–9177.
[8] A. D. Becke, *The Journal of Chemical Physics* 1992, **96**, 2155–2160.
[9] C. Lee, W. Yang, R. G. Parr, *Phys. Rev. B* 1988, **37**, 785–789.
[10] J. S. McNally, B. Noll, C. J. Orme, A. D. Wilson, *J. Phys. Chem. B* 2015, **119**, 6766–6775.
[11] E. F. Pettersen, T. D. Goddard, C. C. Huang, G. S. Couch, D. M. Greenblatt, E. C. Meng, T. E. Ferrin, *Journal of Computational Chemistry* 2004, **25**, 1605–1612.
[12] G. Jogl, X. Wang, S. A. Mason, A. Kovalevsky, M. Mustyakimov, Z. Fisher, C. Hoffman, C. Kratky, P. Langan, *Acta Crystallographica Section D* 2011, **67**, 584–591.
[13] J. Zikovsky, P. F. Peterson, X. P. Wang, M. Frost, C. Hoffmann, *Journal of Applied Crystallography* 2011, **44**, 418–423.
[14] A. J. Schultz, M. R. V. Jørgensen, X. Wang, R. L. Mikkelson, D. J. Mikkelson, V. E. Lynch, P. F. Peterson, M. L. Green, C. M. Hoffmann, *Journal of Applied Crystallography* 2014, **47**, 915–921.
[15] G. M. Sheldrick, *Acta Crystallographica Section C* 2015, **71**, 3–8.
[16] L. J. Farrugia, *Journal of Applied Crystallography* 2012, **45**, 849–854.